DMD Fast Forward. Published on June 7, 2018 as DOI: 10.1124/dmd.118.081596
This article has not been copyedited and formatted. The final version may differ from this version.

Development and Characterisation of a Human Hepatocyte Low Intrinsic Clearance Assay for Use in Drug Discovery

Paul Lancett, Beth Williamson, Patrick Barton & Robert J Riley

Drug Metabolism and Pharmacokinetics, Evotec, 114 Innovation Drive, Milton Park, Abingdon, UK (PL, BW, PB, RJR)

Running Title: Hepatocyte low intrinsic clearance in drug discovery.

Corresponding author: Dr Patrick Barton, Evotec, 114 Innovation Drive, Oxford, OX14 4RZ

Email: patrick.barton@evotec.com

Telephone: +(44) 1235 44 1290

Number of text pages: 32

Number of tables: 3

Number of figures: 4

Number of references: 35

Number of words in Abstract: 250

Number of words in Introduction: 637

Number of words in Discussion: 1318

Abbreviations

18s, ribosomal RNA; ADME, Absorption, Distribution, Metabolism, Excretion; AFE, average fold error; BEH, ethylene bridged hybrid; cDNA, complementary DNA; CL, clearance; CL_{int}, apparent intrinsic clearance; C(t), comparative threshold; CYP, cytochrome P450; DMSO, dimethyl sulfoxide; fu_{inc}, fraction unbound in the incubation; GAPDH, glyceraldehyde-3-phosphate dehydrogenase; GUSB, glucuronidase Beta; HTM, hepatocyte thawing medium; iPSCs, induced pluripotent stem cells; LC-MS/MS, liquid chromatography-tandem mass spectrometry; LLOQ, lower limit of quantification; mRNA, messenger RNA; NCEs, new chemical entities; NR, not reported; PCR, polymerase chain reaction; PHH, primary human hepatocyte; PK, pharmacokinetics; Rb, blood to plasma ratio; RT, reverse transcription; SE,

standard error; TSTAT, T-statistic; UGT, uridine 5'-diphospho-glucuronosyltransferase; WEM, williams E medium.

Abstract

Progression of new chemical entities is a multi-parametric process involving a balance of potency, ADME and safety properties. To accurately predict human pharmacokinetics and estimate human efficacious dose, the use of *in vitro* measures of clearance is often essential. Low metabolic clearance is often targeted to facilitate *in vivo* exposure and achieve appropriate half-life. Suspension primary human hepatocytes (PHH) have been successfully utilised in predictions of clearance. However, incubation times are limited, hindering the limit of quantification. The aims herein were to: evaluate the ability of a novel PHH media supplement, HepExtend™, to maintain cell function, increase culture times and define the clearance of stable compounds. Cell activity was analysed with a range of CYP and uridine 5'-diphospho-glucuronosyltransferase (UGT) substrates and the mRNA expression of drug disposition and toxicity marker genes was determined. HepExtend™ and Geltrex™ were essential to maintain cell activity and viability for 5 days (N=3 donors). In comparison to CM4000±Geltrex™, HepExtend™+Geltrex™ displayed a higher level of gene expression on day 1, particularly for the CYPs, nuclear receptors and UGTs. The novel medium, HepExtend™+Geltrex™, was robust and reproducible in generating statistically significant CL_{int} values at 0.1 µL/min/x10^6 cells over a 30 h period (p <0.05); lower than previously demonstrated. Following regression correction, human hepatic *in vivo* clearance was predicted within 3-fold for 83% of compounds tested for three human donors, with an average fold error of 2.2. The novel PHH medium, HepExtend™, with matrix overlay offers significant improvement for determining compounds with low intrinsic clearance when compared to alternative approaches.

Introduction

A critical practise for the robust design of discovery compounds is the implementation of early absorption, distribution, metabolism and excretion (ADME) assessment. The design process is a multi-parametric process involving a balance of *in vitro* and *in vivo* potency, ADME and safety properties. Early prediction of human pharmacokinetics (PK) can be used to rank compounds to ensure efficient drug design and project progression. To accurately predict human PK and estimate human efficacious dose, measurement of intrinsic clearance (CL_{int}) *in vitro* is a common method for the estimation of human hepatic clearance (CL) (Grime *et al.*, 2013).

Low metabolic CL is often targeted to facilitate *in vivo* exposure and achieve appropriate half-life ($t_{1/2}$) (Riley *et al.*, 2005; Grime and Riley, 2006; Sohlenius-Sternbeck *et al.*, 2012; Di and Obach, 2015). For compounds with moderate volume of distribution (V_{ss}) (~ 2 L/kg) and low CL ($\leq$ 3.5 mL/min/kg), the ability of DMPK scientists to accurately determine *in vitro* CL_{int} is necessary as small changes in CL may have significant impact on the predicted half-life and anticipated human dose (Grime *et al.*, 2013; Bonn *et al.*, 2016).

Suspension primary human hepatocytes (PHHs) containing phase I and phase II metabolising enzymes have been successfully utilised in predictions of compound CL (Riley *et al.*, 2005; Grime and Riley, 2006; Sohlenius-Sternbeck *et al.*, 2012). However, incubation times are limited to 2-4 hours due to declining levels of metabolising activity and an increase in cell mortality, hindering the limit of quantification (Smith *et al.*, 2012). This major limitation has driven the advancement of alternative *in vitro* approaches.

A myriad of alternatives have been evaluated and reviewed by various laboratories (Lau *et al.*, 2002; Novik *et al.*, 2010; Smith *et al.*, 2012; Chan *et al.*, 2013; Di and Obach, 2015; Hutzler *et al.*, 2015). Many share a common goal: to implement more phenotypically relevant models with prolonged metabolising activity to aid *in vivo* hepatic metabolic CL predictions.

The relay method and monolayer/sandwich-cultures of plated PHHs represent two techniques that have been widely appraised for their ability to predict *in vivo* CL of stable compounds (Riley *et al.*, 2005; Grime and Riley, 2006; Di *et al.*, 2012; Peng *et al.*, 2016). Whilst the continuous replenishment of freshly-prepared PHHs overcomes the issue of limited incubation times in suspension assays (Di *et al.*, 2012, 2013), the requirement for substantial volumes of PHHs makes the relay method a labour-intensive approach requiring complex data processing (Di *et al.*, 2012; Hutzler *et al.*, 2015; Peng *et al.*, 2016).

When seeded on collagen-coated plates, PHH viability can be retained for 5 days, and longer with the addition of an overlay, e.g. Geltrex™ (Keemink *et al.*, 2015; Levy *et al.*, 2015). Plating PHHs with an overlay facilitates polarisation of the monolayer, enabling formation of bile canaliculi and localisation of transporters, thus improving the physiologically relevant phenotype (De Bruyn *et al.*, 2013). However, conflicting literature regarding cytochrome P450 3A4 (CYP3A4) and CYP1A2 activities (Smith *et al.*, 2012) suggests further optimisation of this technique is required to ensure optimum metabolic function.

Over the last decade, advances have seen the application of PHHs co-cultured with non-parenchymal cells in 2-D and 3-D culture (Khetani and Bhatia, 2008; Chan *et al.*, 2013; Hutzler *et al.*, 2015; Bonn *et al.*, 2016). Technologies such as HepatoPac® and HμREL™ have been shown to maintain liver-specific drug metabolising enzyme gene expression for up to 6 weeks (Khetani and Bhatia, 2008) and have been successfully utilised for human CL predictions, including stable compounds (Chan *et al.*, 2013; Bonn *et al.*, 2016). However, when contextualised in a discovery setting, co-culture methods do not yet offer the throughput often sought (Hutzler *et al.*, 2015). The same rationale can also be applied to other emerging technologies, including further 3-D models (Chen *et al.*, 2010; Tostões *et al.*, 2011; Godoy *et al.*, 2013) and dynamic flow models (e.g. LiverChip™), which display improved hepatic

physiology and phenotype (Vivares *et al.*, 2015), but are limited by throughput and translation to *in vivo* settings (Hutzler *et al.*, 2015).

Cells derived from induced pluripotent stem cells (iPSCs), e.g. iCell® are an emerging technology that are expected to offer a high-throughput and flexible platform. Initial analysis suggests these cells exhibit hepatic morphology and functions (Rashid *et al.*, 2010; Si-Tayeb *et al.*, 2010; Chen *et al.*, 2012). However, metabolic activities have been reported to be at least ten-fold lower when compared with PHHs. Further investigation is required to understand their optimal application in a discovery setting (Kratochwil *et al.*, 2017). CYP activity levels comparable to PHHs have been purported for the pluripotent cell line HepaRG™ (Turpeinen *et al.*, 2009).

The aims herein were to evaluate the application of a novel plated PHH media supplement, HepExtend™, regarding its ability to maintain cell function, increase culture times and define a lower limit of quantification to improve human hepatic metabolic CL predictions. HepExtend™ was compared to the widely used PHH maintenance medium (CM4000) and the necessity of an overlay for optimal performance was also evaluated.

Materials and Methods

Materials

Primary human hepatocytes (PHH) (Lots Hu1753, Hu8249, Hu1824) were kindly supplied by Thermo Fisher Scientific (Paisley, Scotland). Hepatocyte thawing media (HTM), Primary Hepatocyte Thawing and Plating Supplements (CM3000), Primary Hepatocyte Maintenance Supplements (CM4000), collagen-1 coated 24-well plates, Geltrex™ LDEV-Free Reduced Growth Factor Basement Membrane Matrix (0.35 mg/mL) (a gel matrix additive), HepExtend™ Supplement (50X), reverse transcription reagents, universal master mix, williams E media (WEM), TRIzol® Plus RNA Purification Kit and Taqman gene expression assays were purchased from Thermo Fisher Scientific (Paisley, UK). All other materials were purchased from Sigma-Aldrich (Dorset, UK).

Cryopreserved human hepatocyte cell culture

Plateable cryopreserved PHHs (Table 1) were thawed in HTM and plated in a 24-well collagen-1 coated plate at a density of 3.5 x 10^5 viable cells in 350 µL of WEM/plating supplement. Trypan blue exclusion was used to determine cell viability with a cut-off of 90% viability. The cells were incubated at 37 ^oC in a 95% humidified incubator with 5% CO_2. Plating medium was replaced with WEM/maintenance medium following 4-6 h incubation and then maintained overnight before 30 h treatment with test compound. Each donor was incubated with the following four WEM/maintenance medium:

1. CM4000
2. CM4000+Geltrex™ (described as CM4000+Geltrex from herein)
3. CM4000+HepExtend™ (described as HepExtend from herein)
4. CM4000+HepExtend™+Geltrex™ (described as HepExtend+Geltrex from herein)

Plates were shaken at 50 rpm and samples collected at 0, 1, 2, 4, 8, 22, 26, 30 h. 40 µL samples were quenched in 160 µL of acetonitrile containing 0.1% formic acid and 200 nM of labetalol as internal standard. Samples were shaken for 5 min at 1200 rpm, cooled at -20 ^{o}C for 5 min and centrifuged at 4 ^{o}C for 10 min at 4600 rpm. The supernatant fraction was diluted in an equal volume of water and quantification of parent analysed using liquid chromatography-tandem mass spectrometry (LC-MS/MS).

Following the 30 h compound incubation the cells were carefully washed with WEM/maintenance medium and incubated with fresh WEM/maintenance medium at 37 ^{o}C in a 95% humidified incubator with 5% CO_2 for 48 h before compound treatment was initiated on day 5 following the procedure described above. For gene expression analysis, mRNA was extracted on day 1 or day 5.

Compound Treatment

For comparison of the four medium in the assay a set of reference compounds were selected based on their human CL and *in vitro* intrinsic clearance (CL_{int}) (Table 2). Reference compound CL_{int} ranged from 0.1 - 20 µL/min/x10^6 cells. For all incubations, compounds were dissolved in 100% DMSO to 2 mM, compounds were then diluted to 0.1 mM with acetonitrile:DMSO (91.5:8.5%, respectively). A final compound dilution with maintenance medium was completed to achieve a final DMSO concentration of 0.1% and compound concentration of 1 µM. A vehicle control of medium with 0.1% DMSO was included in all studies.

Determination of intrinsic clearance

Loss of parent compound over the 30 h incubation was used to calculate the *in vitro* CL_{int} on day 1 and day 5 of treatment. Only compounds with a statistically significant CL_{int} (p <0.05) values as defined by the T-statistic were included in the analysis. *In vitro* CL_{int} was transformed

to a predicted human *in vivo* CL_{int} by applying physiological scaling parameters and an incubational binding value (Kilford *et al.,* 2008).

A regression correction method was used to predict *in vivo* CL_{int} as described previously (Sohlenius-Sternbeck *et al.,* 2012). Observed human *in vivo* CL_{int} was calculated using the well-stirred model.

CL_{int} values were scaled to the whole liver by applying physiological scaling factors and incubational binding (fu_{inc}). Fu_{inc} was predicted by applying a non-linear equation as detailed by Kilford *et al.,* 2008. Whilst the equation displays relatively accurate and non-biased results for a range of compounds with LogP <3, the algorithm is based on suspension hepatocytes. Limited data exist to quantify the incubational binding in a plated hepatocyte assay and further work is required to understand this parameter. Nonetheless, similar to previous studies (Bonn *et al.,* 2016), the non-linear equation was applied to the data herein (Figure 1 and 2).

Application of regression correction

The blood-to-plasma ratio (Rb) and fraction unbound was determined previously (Obach *et al.,* 2008; Sohlenius-Sternbeck *et al.,* 2012) however, when no measured Rb value was available, a default value of 0.55 (1-haematocrit) was assumed for acidic compounds and 1 for other ion classes.

To establish the regression line, Log(*in vivo* CL_{int}) was compared to Log(*in vitro* scaled, unbound CL_{int}). The regression correction was then applied to the scaled *in vitro* CL_{int}. From this correction the restricted well-stirred model could be applied to achieve a prediction of *in vivo* CL.

mRNA extraction and reverse transcription

mRNA was extracted from the PHH cell monolayers using the TRIzol® Plus RNA Purification Kit according to manufacturer's instructions. Reverse transcription of mRNA to cDNA was completed using Taqman reverse transcription (RT) assay. RT mixtures were prepared according to manufacturer's instructions; 25 µL reactions consisted of; 10X Taqman RT buffer, $MgCl_2$ (5.49 mM), reverse transcriptase (1 µM), RNA (2 µg), dNTP (50 µM), oligo-d(T) (2.5 µM) and RNase inhibitor (1 µM). An Agilent Mx3005P thermocycler was used to run a thermal cycle of: 10 min at 25 ^{o}C, 30 min at 37 ^{o}C, 5 min at 95 ^{o}C and a hold phase at 4^{o}C.

Quantitative real time-PCR gene expression analysis

An Agilent Mx3005P thermocycler was used to determine the gene expression of 45 selected drug disposition genes plus 3 house-keeping genes (glyceraldehyde-3-phosphate dehydrogenase (GAPDH), glucuronidase beta (GUSB) and ribosomal RNA (18s)) (Supplement Table 1). Real time-PCR Taqman solutions were prepared as described by the manufacturer. Briefly, each reaction contained a 12.5 µL volume; 2X Taqman master mix (6.3 µL), 20X Taqman gene expression assay (0.6 µL), RNase free water (3.6 µL) and 2 µL of cDNA. PCR conditions were 15 min at 95 ^{o}C (to activate polymerase, denature cDNA and initiate PCR) followed by 40 cycles of 15 sec at 94 ^{o}C (denaturation) and 60 sec at 60 ^{o}C (annealing/extension of the product). Fluorescence was measured at the end of each cycle.

No template controls were completed in duplicate to ensure no contamination, specific amplification and maximum amplification, respectively. A geometric mean was used to average the 3 house-keeping controls GAPDH, GUSB, 18s (C(t) values were consistent in every sample). To ensure only gene amplification was measured the C(t) was set to ignore any aberrant fluorescence such as that from primer-dimer formation.

Analysis using LC-MS/MS

LC-MS/MS analysis utilised a triple quadrupole API-4000 mass spectrometer with a Turbo V atmospheric pressure electrospray ionisation source (AB SCIEX, Framingham, MA). All samples (10 µL) were injected onto an ethylene bridged hybrid (BEH) C18 column (2.1 x 30 mm, 1.7 µm) and eluted by a mobile phase gradient specific for each test article (mobile phase A: 0.1% formic acid in water; mobile phase B: 0.1% formic acid in acetonitrile). Flow rate for all compounds was 1.0 mL/min. MS conditions for all compounds: positive or negative ionization mode (5.0 kV spray voltage); source temperature of 450 °C with multiple reaction monitoring specific for each analyte (Supplement Table 2) and internal standard parent-product ion pairs. Peak areas of analyte, and internal standard (labetalol 200 nM) and resulting ratios were quantified using MultiQuant™ Software (AB SCIEX, Framingham, MA).

Data Analysis

All activity data was completed in duplicate for 3 independent experiments (N=3). Gene expression data were compared to an average of GAPDH, GUSB, 18s and normalised to the control sample using the comparative threshold cycle (C(t)) method ($Ct=2^{-\Delta\Delta C(t)}$). Only compounds that produced a statistically significant CL_{int} were included in the analysis. The T-statistic (TSTAT) was applied to determine the significance of the slope:

$$T_{slope} = \frac{Slope}{SE_{slope}}$$

To determine the accuracy of the *in vitro* prediction following application of the regression equation the average fold error (AFE) was calculated between the observed and predicted *in vivo* CL_{int}.

$$AFE = 10^{\frac{1}{N}\sum Log\left(\frac{Observed}{Predicted}\right)}$$

Results

Activity Analysis: Incubations without Geltrex

Day 1

Each donor was treated with a reference compound on day 1 post plating. Initial analysis assessed the activity of each donor following incubation with CM4000 and HepExtend without Geltrex. When incubated with CM4000 or HepExtend all 3 donors generated CL_{int} values following a 30 h compound treatment within 4-fold, except disopyramide and midazolam that displayed a >5-fold difference. However, these CL_{int} values were in agreement between Hu8249 and Hu1753 with the >5-fold discrepancy observed for Hu1824 (Table 3, Figure 1). Hu1824 displayed poor activity for CYP3A4 specific substrates. For each individual donor the CL_{int} values were within 2-fold for each compound regardless of what incubation medium was used (Table 3).

Day 5

Following a 48 h washout period, each donor was treated with a reference compound on day 5 post plating. Initial analysis assessed the activity of each donor following incubation with CM4000 and HepExtend without Geltrex. CL_{int} values obtained following incubation with CM4000 were significantly decreased for Hu1753 compared to day 1 (Table 3). CM4000 was unable to maintain activity for 5 days for all compounds in donors Hu1824 and Hu8249 (Table 3, Figure 1). In comparison, cells incubated with HepExtend generated a CL_{int} value for all 3 donors and the majority of compounds on day 5. However, these values were >2-fold lower when compared to day 1. In contrast to Hu1753 and Hu8249, Hu1824 activity was retained for 36% of compounds (within 2-fold) on day 5 when treated with HepExtend. For all donors treated with CM4000 or HepExtend, a >5-fold decrease in CL_{int} was observed for 61% of compounds on day 5 compared to day 1.

Across all 3 donors, 94% of compounds displayed a >2-fold decrease in CL_{int} from day 1 to day 5. Of these, 76% displayed a >5-fold decrease in CL_{int}.

Activity Analysis: Incubations with Geltrex

Day 1

Each donor was treated with a reference compound on day 1 post plating. Analysis assessed the activity of each donor following incubation with CM4000 and HepExtend with Geltrex. When incubated with CM4000+Geltrex all 3 donors generated CL_{int} values following a 30 h compound treatment within 4-fold, except metoprolol that displayed a 5-fold difference between donors. In comparison to CM4000+Geltrex, activity observed across all 3 donors following HepExtend+Geltrex incubation was relatively consistent. For all compounds and donors a 3-fold difference was observed (excluding imipramine and metoprolol). Hu1753 activity was greater for the CYP1A2 base, imipramine, when incubated with HepExtend+Geltrex compared to the CM4000+Geltrex: 20.6 µL/min/x10^6 cells compared to 8.5 µL/min/x10^6 cells, respectively.

Day 5

Following a 48 h washout period, each donor was treated with a reference compound on day 5 post plating. Analysis assessed the activity of each donor following incubation with CM4000 and HepExtend with Geltrex. Inclusion of an overlay maintained the cells for a longer period so a CL_{int} could be defined on day 5 (Table 3, Figure 1). Further, as shown in Table 3 the addition of Geltrex decreased the fold difference in CL_{int} between day 1 and day 5 for CM4000 and HepExtend.

Following incubation with CM4000+Geltrex, CL_{int} values for 64% of compounds were decreased >2-fold for all 3 donors except carvedilol compared to day 1 (Table 3, Figure 1).

Following incubation with CM4000+Geltrex, CL_{int} values were comparable on day 1 and day 5 for 26% of compounds (≤2-fold across all donors); an improvement of 20% when compared to medium without Geltrex. However, a >5-fold decrease was observed for 16% of compounds. A >5-fold decrease in CL_{int} was observed for midazolam in Hu1753 and Hu8249 and tolbutamide for Hu1824. The decrease was also observed at the mRNA level (Figure 4).

Following incubation with HepExtend+Geltrex, 50% of compounds across all 3 donors produced CL_{int} values within 2-fold on day 1 and day 5 (across all 3 donors) and only 10% displayed a >5-fold decrease in CL_{int} on day 5. For Hu8249 and Hu1753, HepExtend+Geltrex maintained activity for 73% and 64% of compounds (within 2-fold), respectively. In comparison, activity for Hu1824 was only retained for 36% of compounds (within 2-fold).

In comparison to all other donors and culture mediums, Hu8249 produced the most consistent and reproducible CL_{int} values for all experiments (N=3) when incubated with HepExtend+Geltrex (Table 3C, Figure 1). The same trend was observed for the mRNA expression (Figure 4).

mRNA Expression Analysis

Gene expression was assessed on day 1 and day 5 following incubation with the medium. Expression for all genes when incubated with HepExtend+Geltrex on day 1 and day 5 was greater than the reference point of 1 (CM4000+Geltrex), where 1 is equal gene expression (Figure 4A, 4B). Therefore, mRNA expression for all 45 genes was maintained. In comparison to CM4000±Geltrex, HepExtend+Geltrex displayed a higher level of gene expression on day 1, particularly for the CYPs, nuclear receptors and UGTs (Figure 4A). At day 5, the mRNA expression of the hepatic markers (e.g. albumin), the nutritional/metabolic markers (e.g. HMGCS2) (Rescigno *et al.*, 2018), transporters and UGTs were consistent with expression

levels on day 1 (Figure 4B). When compared to Hu1753 and Hu1824, Hu8249 was superior in expressing and subsequently retaining its mRNA expression on day 1 and day 5 when incubated with HepExtend+Geltrex (Figure 4C-F). In contrast, when incubated with HepExtend+Geltrex Hu1753 and Hu1824 expressed higher levels of CYP2C19 compared to Hu8249 (Figure 4C).

Comparison of in vitro to in vivo

In comparison to Hu1753 and Hu1824, activity and mRNA expression for Hu8249 were superior when incubated with HepExtend+Geltrex on day 1 and day 5. This observation justified the selection of this donor to generate a comparison of *in vitro* and *in vivo* data on day 1 (Figure 3).

Similar to previous studies (Sohlenius-Sternbeck *et al.*, 2012), the *in vitro* data under-predicted the *in vivo* CL hence, a regression correction was required (Figure 3B). Following regression correction, human hepatic *in vivo* CL was predicted within 3-fold for 83% of compounds tested for Hu8249, with an average fold error (AFE) of 2.2. No significant difference was observed between values as determined by the Bland-Altman analysis (Bias $8x10^{-4}$, 95% CI −0.82 and 0.82).

Despite the chemical instability observed in media-only incubations (Figure 2C, D), *in vitro* data generated for bupropion correlated with the *in vivo* observation (Figure 3). The hepatocyte CL_{int} was greater than 10-fold higher than the media-only CL_{int}, suggesting the impact of chemical instability on the *in vivo* CL_{int} prediction is negligible. However, the observation is nonetheless noteworthy, and a worthwhile consideration in the context of ensuring accuracy in human predictions.

Diclofenac and tolbutamide fell outside the 2-fold lines of agreement (>3-fold) (Figure 3B). These outliers have been reported previously (Hewitt and Utesch, 2004; Chan *et al.*, 2013).

Cryopreservation techniques have been noted to alter CYP2C9 activity and this could contribute to the off-set observed for tolbutamide (Hewitt and Utesch, 2004).

Discussion

Metabolically stable compounds present a challenge in drug discovery due to the quantification limits of existing hepatocyte suspension assays (Smith *et al.*, 2012). Defining human hepatic metabolic CL_{int} *in vitro* is key for scaling to *in vivo* human CL; arguably the key parameter in predicting human PK and estimating efficacious dose (Grime *et al.*, 2013). Noting this limitation, work herein was focused on optimising an assay to define the CL_{int} for metabolically stable project compounds.

Following a review of the literature (Lau *et al.*, 2002; Novik *et al.*, 2010; Di *et al.*, 2012; Smith *et al.*, 2012; Chan *et al.*, 2013; Hutzler *et al.*, 2015), plated PHHs were chosen as a method for determining human CL_{int} values less than 3 µL/min/x10^6 cells. The media supplements HepExtend™ and Geltrex™ were compared to the widely-used PHH maintenance medium, CM4000, to determine their effectiveness in extending CYP function beyond the reported 10 hours (Smith *et al.*, 2012; Bonn *et al.*, 2016). Additionally, the utility of the supplements plus an overlay for prolonging cell function after 5 days in culture was assessed.

In contrast to previous work (Hutzler *et al.*, 2015; Bonn *et al.*, 2016), reproducible linear CL_{int} profiles for disopyramide and warfarin were generated throughout the analysis. A no cell control further confirmed the robustness of the assay and the ability to generate a statistically significant CL_{int} of 0.1 µL/min/x10^6 cells (Figure 1).

Geltrex™ prolonged metabolising enzyme function, with day 5 CL_{int} values significantly lower than day 1 in the assays without Geltrex™ (76% and 61% displayed a >5-fold decrease in CL_{int} for reference compounds with CM4000 and HepExtend, respectively). An additional improvement in maintaining metabolic CL rates was observed with the presence of HepExtend™. Incubations containing both supplements generated CL_{int} values most comparable to day 1 (50% of CL_{int} values were within 2-fold for all three donors).

The effectiveness of the supplement was donor-specific, with Hu8249 benefitting the most (Table 3, Figure 2). For example, 91% of compounds tested on both days deviated less than 3-fold in the presence of both media supplements. This finding presents discovery teams with the potential to use the same hepatocyte cultures for two separate assays, offering both cost and time-saving benefits. However, characterisation is required to ensure hepatocyte function is maintained for individual donors for up to 5 days, while the potential impact of suicide inhibitors should also be considered.

At a gene level, expression of uptake and efflux transporters, CYPs, UGTs and nuclear receptors in Hu8249 were enhanced on both day 1 and day 5 when HepExtend™ was in the culture media (Figure 4). This highlights the functional benefits of including HepExtend™ and Geltrex™ in monolayer cultures. It is hypothesised HepExtend™ provides additional hepatocyte nutrients for improved function, while Geltrex™ provides the support for enhanced cell to cell contact and subsequent morphology.

CL_{int} was successfully determined for low-turnover compounds, with statistically-significant values (p <0.05) measured repeatedly for disopyramide, diazepam, metoprolol and tolbutamide (Table 3, Figure 2). Some laboratories define the lower limit of quantification (LLOQ) by extrapolating the incubation time, for example, a 10 hour incubation can produce an LLOQ CL_{int} of 0.5 µL/min/x10^6 cells (Bonn *et al.*, 2016). Alternatively, LLOQ can be defined by the lowest possible statistically-significant CL_{int} as determined from TSTAT analysis (e.g. 30 hour incubation = 0.1 µL/min/x10^6 cells, as defined herein). Furthermore, the log-linear substrate depletion profiles remain linear for up to 30 hours (Figure 1). Consequently, the LLOQ of this assay is lower than other laboratories have reported using plated PHHs (Bonn *et al.*, 2016). Further, Hutzler *et al* (2015) suggested that incubations for CL estimation should be limited to 24 hours or less. A key differentiator between our assay and others is the inclusion of additional supplements in the maintenance media.

After 1 day in culture, PHH activity was similar for each donor and each culture medium (Table 3). This demonstrated that metabolising enzyme function and activity was not impaired by the presence of HepExtend and/or Geltrex when the cells were used within 48 hours of plating. Additionally, for Hu8249 mRNA analysis confirmed an increase in mRNA expression for all 45 genes (Figure 4).

Out of the 3 donors characterised, Hu1824 had noticeably lower activity than Hu1753 and Hu8249, particularly for CYP3A4 and its substrate midazolam. This may be explained at a gene level, with lower quantities of mRNA quantifiable at day 1 and day 5 in comparison to Hu1753 and Hu8249 (Figure 4). These observations illustrate the importance of donor characterisation, and the requirement to batch test donors prior to use in drug discovery (Hutzler *et al.*, 2014), and define a donor-specific regression (Sohlenius-Sternbeck *et al.*, 2012).

Extrapolation of *in vitro* stability data using physiological scaling parameters, including fu_{inc} correction (Austin *et al.*, 2005; Kilford *et al.*, 2008), and the restricted well-stirred model resulted in a systematic under-prediction of CL. This systematic bias was removed by applying an empirical regression correction to the *in vitro* data for the defined set of reference compounds (Figure 3). Following regression correction, human hepatic *in vivo* CL was predicted within 3-fold for 83% of compounds tested for the 3 human donors, with an average fold error (AFE) of 2.2. Subsequently, applying the same regression corrections to drug discovery compounds can improve CL predictions from *in vitro* metabolism data, and ultimately lead to improved PK predictions (Riley *et al.*, 2005; Sohlenius-Sternbeck *et al.*, 2012). However, it should be noted that the root cause of the inaccuracies inherent in the regression approach remain undefined (Bowman and Benet, 2016).

Where possible, all human donors should provide representation of all drug metabolising activity. For example, Hu1824 demonstrated low CYP3A4 activity, which would result in this

donor under-predicting human CL for all compounds where the fraction metabolised by CYP3A4 is significant. Thus, a regression correction would not mitigate against the reduced activity of the isoform. This observation reinforces the importance of characterising human donors prior to use in drug discovery screens. Additionally, under-predictions of *in vivo* CL can be accentuated in PHHs when compounds are highly cleared, possibly due to rate-limited uptake of compound into static flow hepatocyte monolayers, and the reduced surface area for drug diffusion relative to suspension assays, impacting apparent enzyme kinetics (Hutzler *et al*., 2015).

As an alternative to single donors, development of pooled human donors suitable for plating have received much attention, with the purpose of improving human CL predictions by overcoming population differences. Pools of human hepatocytes in suspension cultures have been widely utilised (Shibata *et al.*, 2002; Riley *et al.*, 2005; Grime and Riley, 2006; Sohlenius-Sternbeck *et al.*, 2012; Hutzler *et al.*, 2015) while historically, pooled donors in plated monocultures have proved far more challenging, with some donors not amenable to plating (Hutzler *et al.*, 2015). Technology is continuing to improve in this area, with suppliers now offering plateable donor pools verified for Phase I enzyme activity and plating efficiency. The authors acknowledge the value of these products, not only to account for poor metabolisers, but also for variances driven by uptake rates of transporter substrates. However, the robust nature of our validation for single human donors, including the use of isoform-specific markers and donor-specific regression correction, provide us with confidence in our chosen donor(s) and their utility for providing physiologically-relevant hepatic metabolism rates.

For this validation, the compound selection focused on representing a range of CYP isoforms. While CYPs are responsible for metabolic elimination of the majority of drugs currently on the market (Williams *et al.*, 2004), we recognise the importance of not limiting donor validations solely to CYPs. UGTs also constitute an important group of conjugating enzymes, and

representative markers including ethinyl estradiol (UGT1A1) and zidovudine (UGT2B7) have since been included in our validation sets (full dataset not shown).

After applying the regression correction (Figure 3), diclofenac and tolbutamide were identified as outliers (greater than 3-fold outside the line of unity). Pertinent to diclofenac, literature reports suggest variance in CL predictions can be accentuated for high CL compounds (Hutzler *et al.*, 2015). Furthermore, cryopreservation techniques have been noted to alter CYP2C9 activity and this could contribute to the off-sets observed for both compounds (Hewitt and Utesch, 2004; Brown *et al.*, 2007).

In summary, a plated hepatocyte assay capable of quantifying stable compounds and thus improving the precision of human *in vivo* CL predictions has been developed. This assay enables generation of linear substrate depletion profiles for up to 30 hours, providing reliable CL_{int} values as low as 0.1 µL/min/x10^6 cells. With the addition of a regression correction, *in vivo* CL predictions within 3-fold of observed CL for 83% of our diverse substrate selection were derived. More work is required to validate the approach for non-CYP metabolic CL mechanisms. With the inclusion of media supplements HepExtend™ and Geltrex™, the same hepatocyte cultures have the potential to be used for two separate assays. With a cautionary note of suicide inhibitors for new chemical entities this assay could offer significant cost and time-saving benefits to drug discovery groups.

Acknowledgments

The authors would like to acknowledge Thermo Fisher Scientific: Life Technologies for providing the primary human hepatocytes.

Author Contributions

Participated in research design: Barton, Riley, Williamson

Conducted experiments: Lancett, Williamson

Performed data analysis: Lancett, Williamson

Wrote or contributed to the writing of the manuscript: Barton, Lancett, Riley, Williamson

References

Bonn B, Svanberg P, Janefeldt A, Hultman I, and Grime K (2016) Determination of Human Hepatocyte Intrinsic Clearance for Slowly Metabolized Compounds: Comparison of a Primary Hepatocyte/Stromal Cell Co-culture with Plated Primary Hepatocytes and HepaRG. *Drug Metab Dispos* **44**:527 LP-533.

Brown HS, Griffin M, and Houston JB (2007) Evaluation of Cryopreserved Human Hepatocytes as an Alternative in Vitro System to Microsomes for the Prediction of Metabolic Clearance. *Drug Metab Dispos* **35**:293 LP-301.

Chan TS, Yu H, Moore A, Khetani SR, and Tweedie D (2013) Meeting the Challenge of Predicting Hepatic Clearance of Compounds Slowly Metabolized by Cytochrome P450 Using a Novel Hepatocyte Model, HepatoPac. *Drug Metab Dispos* **41**:2024 LP-2032.

Chen GC, Ramanathan VS, Law D, Funchain P, Chen GC, French S, Shlopov B, Eysselein V, Chung D, Reicher S, and Pham B V (2010) Acute liver injury induced by weight-loss herbal supplements. *World J Hepatol* **2**:410–415, Baishideng Publishing Group Co., Limited.

Chen Y-F, Tseng C-Y, Wang H-W, Kuo H-C, Yang VW, and Lee OK (2012) Rapid generation of mature hepatocyte-like cells from human induced pluripotent stem cells by an efficient three-step protocol. *Hepatology* **55**:1193–1203, Wiley Subscription Services, Inc., A Wiley Company.

De Bruyn T, Chatterjee S, Fattah S, Keemink J, Nicolaï J, Augustijns P, and Annaert P (2013) Sandwich-cultured hepatocytes: utility for in vitro exploration of hepatobiliary drug disposition and drug-induced hepatotoxicity. *Expert Opin Drug Metab Toxicol* **9**:589–616.

Di L, Atkinson K, Orozco CC, Funk C, Zhang H, McDonald TS, Tan B, Lin J, Chang C, and Obach RS (2013) In Vitro–In Vivo Correlation for Low-Clearance Compounds Using

Hepatocyte Relay Method. *Drug Metab Dispos* **41**:2018 LP-2023.

Di L, and Obach RS (2015) Addressing the Challenges of Low Clearance in Drug Research. *AAPS J* **17**:352–357, Springer US, Boston.

Di L, Trapa P, Obach RS, Atkinson K, Bi Y-A, Wolford AC, Tan B, McDonald TS, Lai Y, and Tremaine LM (2012) A Novel Relay Method for Determining Low-Clearance Values. *Drug Metab Dispos* **40**:1860 LP-1865.

Godoy P, Hewitt NJ, Albrecht U, Andersen ME, Ansari N, Bhattacharya S, Bode JG, Bolleyn J, Borner C, Böttger J, Braeuning A, Budinsky RA, Burkhardt B, Cameron NR, Camussi G, Cho C-S, Choi Y-J, Craig Rowlands J, Dahmen U, Damm G, Dirsch O, Donato MT, Dong J, Dooley S, Drasdo D, Eakins R, Ferreira KS, Fonsato V, Fraczek J, Gebhardt R, Gibson A, Glanemann M, Goldring CEP, Gómez-Lechón MJ, Groothuis GMM, Gustavsson L, Guyot C, Hallifax D, Hammad S, Hayward A, Häussinger D, Hellerbrand C, Hewitt P, Hoehme S, Holzhütter H-G, Houston JB, Hrach J, Ito K, Jaeschke H, Keitel V, Kelm JM, Kevin Park B, Kordes C, Kullak-Ublick GA, LeCluyse EL, Lu P, Luebke-Wheeler J, Lutz A, Maltman DJ, Matz-Soja M, McMullen P, Merfort I, Messner S, Meyer C, Mwinyi J, Naisbitt DJ, Nussler AK, Olinga P, Pampaloni F, Pi J, Pluta L, Przyborski SA, Ramachandran A, Rogiers V, Rowe C, Schelcher C, Schmich K, Schwarz M, Singh B, Stelzer EHK, Stieger B, Stöber R, Sugiyama Y, Tetta C, Thasler WE, Vanhaecke T, Vinken M, Weiss TS, Widera A, Woods CG, Xu JJ, Yarborough KM, and Hengstler JG (2013) Recent advances in 2D and 3D in vitro systems using primary hepatocytes, alternative hepatocyte sources and non-parenchymal liver cells and their use in investigating mechanisms of hepatotoxicity, cell signaling and ADME. *Arch Toxicol* **87**:1315–1530, Springer Berlin Heidelberg, Berlin/Heidelberg.

Grime K, and Riley RJ (2006) The Impact of In Vitro Binding on In Vitro - In Vivo Extrapolations, Projections of Metabolic Clearance and Clinical Drug-Drug Interactions.

Curr Drug Metab **7**:251–264.

Grime KH, Barton P, and McGinnity DF (2013) Application of In Silico, In Vitro and Preclinical Pharmacokinetic Data for the Effective and Efficient Prediction of Human Pharmacokinetics. *Mol Pharm* **10**:1191–1206, American Chemical Society.

Hewitt NJ, and Utesch D (2004) Cryopreserved rat, dog and monkey hepatocytes: measurement of drug metabolizing enzymes in suspensions and cultures. *Hum Exp Toxicol* **23**:307–316.

Hutzler JM, Ring BJ, and Anderson SR (2015) Low-Turnover Drug Molecules: A Current Challenge for Drug Metabolism Scientists. *Drug Metab Dispos* **43**:1917 LP-1928.

Hutzler JM, Yang Y-S, Brown C, Heyward S, and Moeller T (2014) Aldehyde Oxidase Activity in Donor-Matched Fresh and Cryopreserved Human Hepatocytes and Assessment of Variability in 75 Donors. *Drug Metab Dispos* **42**:1090 LP-1097.

Keemink J, Oorts M, and Annaert P (2015) Primary hepatocytes in sandwich culture, in *Protocols in In Vitro Hepatocyte Research* pp 175–188.

Khetani SR, and Bhatia SN (2008) Microscale culture of human liver cells for drug development. *Nat Biotech* **26**:120–126, Nature Publishing Group.

Kilford PJ, Gertz M, Houston JB, and Galetin A (2008) Hepatocellular Binding of Drugs: Correction for Unbound Fraction in Hepatocyte Incubations Using Microsomal Binding or Drug Lipophilicity Data. *Drug Metab Dispos* **36**:1194 LP-1197.

Kratochwil NA, Meille C, Fowler S, Klammers F, Ekiciler A, Molitor B, Simon S, Walter I, McGinnis C, Walther J, Leonard B, Triyatni M, Javanbakht H, Funk C, Schuler F, Lavé T, and Parrott NJ (2017) Metabolic Profiling of Human Long-Term Liver Models and Hepatic Clearance Predictions from In Vitro Data Using Nonlinear Mixed-Effects Modeling. *AAPS J* **19**:534–550.

Lau YY, Sapidou E, Cui X, White RE, and Cheng K-C (2002) Development of a Novel in

Vitro Model to Predict Hepatic Clearance Using Fresh, Cryopreserved, and Sandwich-Cultured Hepatocytes. *Drug Metab Dispos* **30**:1446 LP-1454.

Levy G, Bomze D, Heinz S, Ramachandran SD, Noerenberg A, Cohen M, Shibolet O, Sklan E, Braspenning J, and Nahmias Y (2015) Long-term culture and expansion of primary human hepatocytes. *Nat Biotechnol* **33**:1264–1271.

Novik E, Maguire TJ, Chao P, Cheng KC, and Yarmush ML (2010) A microfluidic hepatic coculture platform for cell-based drug metabolism studies. *Biochem Pharmacol* **79**:1036–1044.

Obach RS, Lombardo F, and Waters NJ (2008) Trend analysis of a database of intravenous pharmacokinetic parameters in humans for 670 drug compounds. *Drug Metab Dispos* **36**:1385–1405.

Peng C-C, Doshi U, Prakash C, and Li AP (2016) A Novel Plated Hepatocyte Relay Assay (PHRA) for In Vitro Evaluation of Hepatic Metabolic Clearance of Slowly Metabolized Compounds. *Drug Metab Lett* **10**:3–15.

Rashid ST, Corbineau S, Hannan N, Marciniak SJ, Miranda E, Alexander G, Huang-Doran I, Griffin J, Ahrlund-Richter L, Skepper J, Semple R, Weber A, Lomas DA, and Vallier L (2010) Modeling inherited metabolic disorders of the liver using human induced pluripotent stem cells. *J Clin Invest* **120**:3127–3136, The American Society for Clinical Investigation.

Rescigno T, Capasso A, and Tecce MF (2018) Involvement of nutrients and nutritional mediators in mitochondrial 3-hydroxy-3-methylglutaryl-CoA synthase gene expression. *J Cell Physiol* **233**:3306–3314.

Riley RJ, McGinnity DF, and Austin RP (2005) A unified model for predicting human hepatic, metabolic clearance from in vitro intrinsic clearance data in hepatocytes and microsomes. *Drug Metab Dispos* **33**:1304–1311.

Shibata Y, Takahashi H, Chiba M, and Ishii Y (2002) Prediction of Hepatic Clearance and Availability by Cryopreserved Human Hepatocytes: An Application of Serum Incubation Method. *Drug Metab Dispos* **30**:892 LP-896.

Si-Tayeb K, Noto FK, Nagaoka M, Li J, Battle MA, Duris C, North PE, Dalton S, and Duncan SA (2010) Highly Efficient Generation of Human Hepatocyte–like Cells from Induced Pluripotent Stem Cells. *Hepatology* **51**:297–305.

Smith CM, Nolan CK, Edwards MA, Hatfield JB, Stewart TW, Ferguson SS, Lecluyse EL, and Sahi J (2012) A comprehensive evaluation of metabolic activity and intrinsic clearance in suspensions and monolayer cultures of cryopreserved primary human hepatocytes. *J Pharm Sci* **101**:3989–4002.

Sohlenius-Sternbeck A-K, Jones C, Ferguson D, Middleton BJ, Projean D, Floby E, Bylund J, and Afzelius L (2012) Practical use of the regression offset approach for the prediction of in vivo intrinsic clearance from hepatocytes. *Xenobiotica* **42**:841–853, Taylor & Francis.

Tostões RM, Leite SB, Miranda JP, Sousa M, Wang DIC, Carrondo MJT, and Alves PM (2011) Perfusion of 3D encapsulated hepatocytes—A synergistic effect enhancing long-term functionality in bioreactors. *Biotechnol Bioeng* **108**:41–49, Wiley Subscription Services, Inc., A Wiley Company.

Turpeinen M, Tolonen A, Chesne C, Guillouzo A, Uusitalo J, and Pelkonen O (2009) Functional expression, inhibition and induction of CYP enzymes in HepaRG cells. *Toxicol Vitr* **23**:748–753.

Vivares A, Salle-Lefort S, Arabeyre-Fabre C, Ngo R, Penarier G, Bremond M, Moliner P, Gallas J-F, Fabre G, and Klieber S (2015) Morphological behaviour and metabolic capacity of cryopreserved human primary hepatocytes cultivated in a perfused multiwell device. *Xenobiotica* **45**:29–44, Taylor & Francis.

Williams JA, Hyland R, Jones BC, Smith DA, Hurst S, Goosen TC, Peterkin V, Koup JR, and Ball SE (2004) Drug-drug interactions for UDP-glucuronosyltransferase substrates: A pharmacokinetic explanation for typically observed low exposure (AUC 1/AUC) ratios. *Drug Metab Dispos* **32**:1201–1208.

Footnote

The two first authors made equal contributions to this publication.

Figure Legends

Figure 1. Comparison of donor intrinsic clearance scaled to the whole liver for each medium on day 1 (A, C, E, G) and day 5 (B, D, F, H).

A+B: CM4000, C+D: CM4000+Geltrex, E+F: HepExtend, G+H: HepExtend+Geltrex. Each bar represents the mean and standard deviation of 3 independent experiments. Bland Altman analysis was completed to compare medium influence on day 1 and day 5. CM4000; Hu1753 Bias 20.6, 95% CI -15.0-56.2; Hu1824 and Hu8249 not applicable. CM4000+Geltrex; Hu1753 Bias 37.2, 95% CI -28.1-102.5, Hu1824 Bias 18.4, 95% CI -56.3-93.0, Hu8249 Bias 28.5, 95% CI -38.8-95.8. HepExtend; Hu1753 Bias 19.5, 95% CI -23.4-62.3, Hu1824 Bias 13.5, 95% CI -6.6-33.6, Hu8249 Bias 15.5, 95% CI -15.9-46.9. HepExtend+Geltrex; Hu1753 Bias 27.7, 95% CI -89.9-145.4, Hu1824 Bias 9.6, 95% CI -12.6-31.8, Hu8249 Bias 7.4, 95% CI -6.0-20.6.

Figure 2. Substrate depletion plot for Hu8249. Cells treated with A) disopyramide and C) bupropion with CM4000+Geltrex on day 1 and media alone with B) disopyramide and D) bupropion.

Where, the CL_{int} for disopyramide with cells was 0.19 µL/min/x10^6 cells, $p = 1.5x10^{-5}$ and the CL_{int} for disopyramide with media only was < 0.1 µL/min/x10^6 cells, $p > 0.05$. CL_{int} for bupropion with cells was 6.4 µL/min/x10^6 cells, $p = 4.6x10^{-3}$ and the CL_{int} for bupropion with media only was 0.47 µL/min/x10^6 cells, $p = 4.5x10^{-6}$.

Figure 3. Comparison of *in vitro* and *in vivo* CL_{int} for compounds detailed in Table 2 before a regression correction (A) and following regression correction (B).

A comparison of the *in vitro* and *in vivo* values was completed using Bland-Altman: Bias $8x10^{-4}$, 95% CI: -0.82-0.82, average fold error 2.2.

Where, the dotted line represents unity on both plots and the solid lines represents the regression line in (A) and a ±2-fold offset from unity in (B).

Figure 4. Comparison of mRNA expression on assay day 1 and day 5.

Change in relative gene expression for Hu8249 when normalised to CM4000+Geltrex Day 1 for major drug disposition genes (Supplement Table 1) (A, B). Relative gene expression of Hu1753 and Hu1824 when normalised to Hu8249 on day 1 (C, D) and day 5 (E, F) for major drug disposition genes (Supplement Table 1).

Tables

Donor demographics

Donor	Ethnicity	Gender	Age	BMI	Tobacco History	Alcohol History	Drug History	Medications
Hu1753	Caucasian	Female	43	22	Yes	Yes	None reported	Scopolamine patch, 1.5mg transdermal q 72h prn
Hu1824	Caucasian	Female	66	28	Yes	No	None reported	None reported
Hu8249	African American	Male	29	22	Yes	Yes	Yes	None reported

Table 1. Human donor demographics of the hepatocytes used in the study.

DMD Fast Forward. Published on June 7, 2018 as DOI: 10.1124/dmd.118.081596
This article has not been copyedited and formatted. The final version may differ from this version.

Overview of the validation compounds used in the analysis

Compound	**Metabolising Enzymes**	**Chemical Class**	**LogD/P**	**Human fu_p**	**Human *in vivo* CL (mL/min/Kg)**
Bupropion	CYP2B6, CYP1A2, CYP2A6, CYP3A4, CYP2E1	Base	3.27	0.15	10.45
Carvedilol	CYP2D6, CYP2C9	Base	3.42	0.02	7.80
Diazepam	CYP2C19, CYP3A4	Neutral	2.8	0.023	0.38
Diclofenac	CYP2C9, UGT2B7	Acid	1.12	0.005	4.20
Disopyramide	CYP3A4	Base	2.58	0.16	0.90
Ethinyl Estradiol	UGT1A1, CYP3A4	Acid	4.11	0.01	5.0
Imipramine	CYP1A2, CYP2C19, CYP2D6	Base	4.28	0.075	9.50
Metoprolol	CYP2D6, CYP3A4	Base	1.76	0.88	13.30
Midazolam	3A4	Neutral	3.4	0.017	4.60
Sildenafil	CYP3A4, CYP2C9, CYP2C19	Base	2.8	0.04	6.00
Tolbutamide	2C9	Acid	0.47	0.05	0.17
Warfarin	CYP2C9, CYP3A4	Neutral	0.2	0.015	0.05

Table 2. Physicochemical properties and human clearance values for the compounds included in the analysis (Sohlenius-Sternbeck *et al.*, 2012; Chan *et al.*, 2013; Hutzler *et al.*, 2015). Where, fu_p is fraction unbound in the plasma, LogD is the distribution coefficient and LogP is the partition coefficient. LogD is quoted for acids and neutrals and LogP for bases.

DMD Fast Forward. Published on June 7, 2018 as DOI: 10.1124/dmd.118.081596
This article has not been copyedited and formatted. The final version may differ from this version.

Stability results for each donor following incubation in different culture medium

A **Hu1753**

	CM4000 CL_{int} (µL/min/×10^6 cells)			HepExtend CL_{int} (µL/min/×10^6 cells)			CM4000+Geltrex CL_{int} (µL/min/×10^6 cells)			HepExtend+Geltrex CL_{int} (µL/min/×10^6 cells)		
Compound	**Day 1**	**Day 5**	**Fold-Shift**	**Day 1**	**Day 5**	**Fold-Shift**	**Day 1**	**Day 5**	**Fold-Shift**	**Day 1**	**Day 5**	**Fold-Shift**
Bupropion	3.3	0.9	-3.7	3.4	0.4	-8.6	4.6	ND	NA	ND	ND	NA
Carvedilol	12.1	6.7	-1.8	8.9	1.3	-6.9	14.5	11.1	-1.3	14.3	12.7	-1.1
Diazepam	0.8	0.1	-6.9	1.8	*	NA	0.7	0.2	-3.8	0.6	*	NA
Diclofenac	4.5	1.4	-3.2	1.3	0.2	-6.9	4.7	2.8	-1.7	1.5	4.2	2.9
Disopyramide	0.10	*	NA	*	*	NA	0.1	*	NA	0.1	*	NA
Imipramine	5.8	1.0	-5.6	5.3	0.2	-24.5	8.5	2.0	-4.2	20.6	4.3	-4.8
Metoprolol	0.6	0.1	-6.5	0.5	*	NA	0.9	0.7	-1.3	0.9	1.3	1.4
Midazolam	5.3	0.9	-6.0	6.1	*	NA	5.1	0.6	-8.4	6.7	4.1	-1.6
Sildenafil	5.5	0.6	-8.8	4.0	*	NA	7.1	2.9	-2.4	7.3	3.2	-2.3
Tolbutamide	1.7	0.2	-10.6	1.3	*	NA	0.8	0.5	-1.6	0.5	2.6	5.5
Warfarin	*	0.1	NA	*	*	NA	0.3	*	NA	*	*	NA

B **Hu1824**

	CM4000 CL_{int} (µL/min/×10^6 cells)			HepExtend CL_{int} (µL/min/×10^6 cells)			CM4000+Geltrex CL_{int} (µL/min/×10^6 cells)			HepExtend + Geltrex CL_{int} (µL/min/×10^6 cells)		
Compound	**Day 1**	**Day 5**	**Fold-Shift**	**Day 1**	**Day 5**	**Fold-Shift**	**Day 1**	**Day 5**	**Fold-Shift**	**Day 1**	**Day 5**	**Fold-Shift**
Bupropion	3.3	*	NA	4.3	1.04	-4.2	2.7	1.3	-2.0	3.1	1.5	-2.1
Carvedilol	14.6	*	NA	14.2	3.10	-4.6	9.3	6.3	-1.5	6.9	6.4	-1.1
Diazepam	0.2	*	NA	*	0.65	NA	0.3	*	NA	0.4	0.2	-2.4
Diclofenac	3.2	*	NA	2.1	0.64	-3.2	3.4	1.4	-2.4	1.6	0.8	-1.9
Disopyramide	<0.1	*	NA	*	*	NA	*	*	NA	NA	*	NA
Imipramine	1.0	*	NA	ND	1.40	NA	2.8	1.1	-2.5	3.9	1.1	-3.7
Metoprolol	0.2	*	NA	0.4	*	NA	0.2	0.2	-1.1	0.2	0.1	-1.4
Midazolam	0.7	*	NA	1.9	1.17	-1.6	ND	0.4	NA	ND	*	NA
Sildenafil	2.7	*	NA	2.0	1.06	-1.9	3.4	0.7	-4.6	3.3	1.1	-3.0

DMD Fast Forward. Published on June 7, 2018 as DOI: 10.1124/dmd.118.081596
This article has not been copyedited and formatted. The final version may differ from this version.

Tolbutamide	0.5	*	NA	0.2	0.31	1.3	0.7	*	NA	0.5	*	NA
Warfarin	0.1	*	NA	*	0.18	NA	0.1	*	NA	*	*	NA

C **Hu8249**

	CM4000 CL_{int} (µL/min/×10^6 cells)			**HepExtend CL_{int} (µL/min/×10^6 cells)**			**CM4000 + Geltrex CL_{int} (µL/min/×10^6 cells)**			**HepExtend + Geltrex CL_{int} (µL/min/×10^6 cells)**		
Compound	**Day 1**	**Day 5**	**Fold-Shift**	**Day 1**	**Day 5**	**Fold-Shift**	**Day 1**	**Day 5**	**Fold-Shift**	**Day 1**	**Day 5**	**Fold-Shift**
Bupropion	7.5	*	NA	7.1	2.41	-2.9	5.4	1.6	-3.3	5.7	2.7	-2.1
Carvedilol	17.4	*	NA	14.6	7.13	-2.1	13.1	13.9	1.1	8.2	8.1	-1.0
Diazepam	1.0	*	NA	0.5	0.35	-1.5	1.0	*	NA	0.9	0.3	-3.0
Diclofenac	4.2	*	NA	1.6	1.21	-1.4	4.2	1.8	-2.4	3.3	1.2	-2.7
Disopyramide	0.3	*	NA	*	*	NA	0.3	*	NA	0.2	0.1	-1.6
Ethinyl Estradiol	ND	ND	NA	ND	ND	ND	ND	ND	ND	3.3	ND	NA
Imipramine	4.9	*	NA	ND	1.07	NA	2.5	0.5	-4.8	4.0	2.2	-1.8
Metoprolol	0.6	*	NA	0.7	0.32	-2.2	0.5	0.3	-1.5	0.5	0.5	-1.2
Midazolam	9.4	*	NA	12.4	1.43	-8.6	7.6	1.3	-5.7	6.2	3.7	-1.7
Sildenafil	12.3	*	NA	16.8	*	NA	10.0	2.6	-3.9	7.7	4.4	-1.8
Tolbutamide	1.0	*	NA	0.5	*	NA	0.9	*	NA	0.8	0.3	-2.5
Warfarin	0.1	*	NA	*	*	NA	0.1	*	NA	0.2	*	NA

Table 3. *In vitro* intrinsic clearance (CL_{int}) and the fold change in CL_{int} for each donor and medium tested on assay day 1 and assay day 5: A, Hu1753; B, Hu1824; C, Hu8249.

Where, each value is the mean of N=3, * represents no statistically significant CL_{int}, ND is not determined due to cell death or the compound was not included in the analysis, NA is not applicable.

DMD Fast Forward. Published on June 7, 2018 as DOI: 10.1124/dmd.118.081596
This article has not been copyedited and formatted. The final version may differ from this version.

Figures

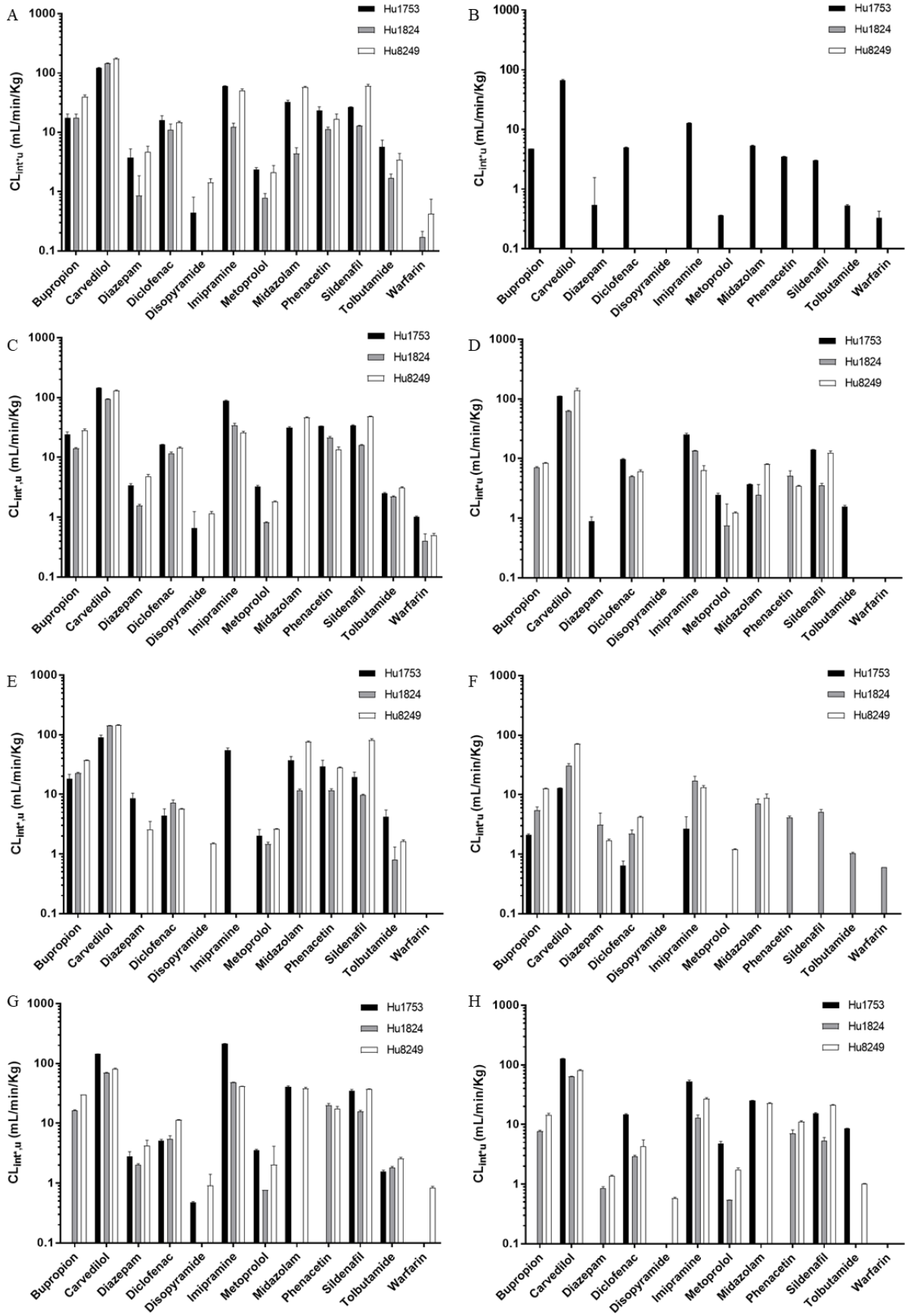

Figure 1

DMD Fast Forward. Published on June 7, 2018 as DOI: 10.1124/dmd.118.081596
This article has not been copyedited and formatted. The final version may differ from this version.

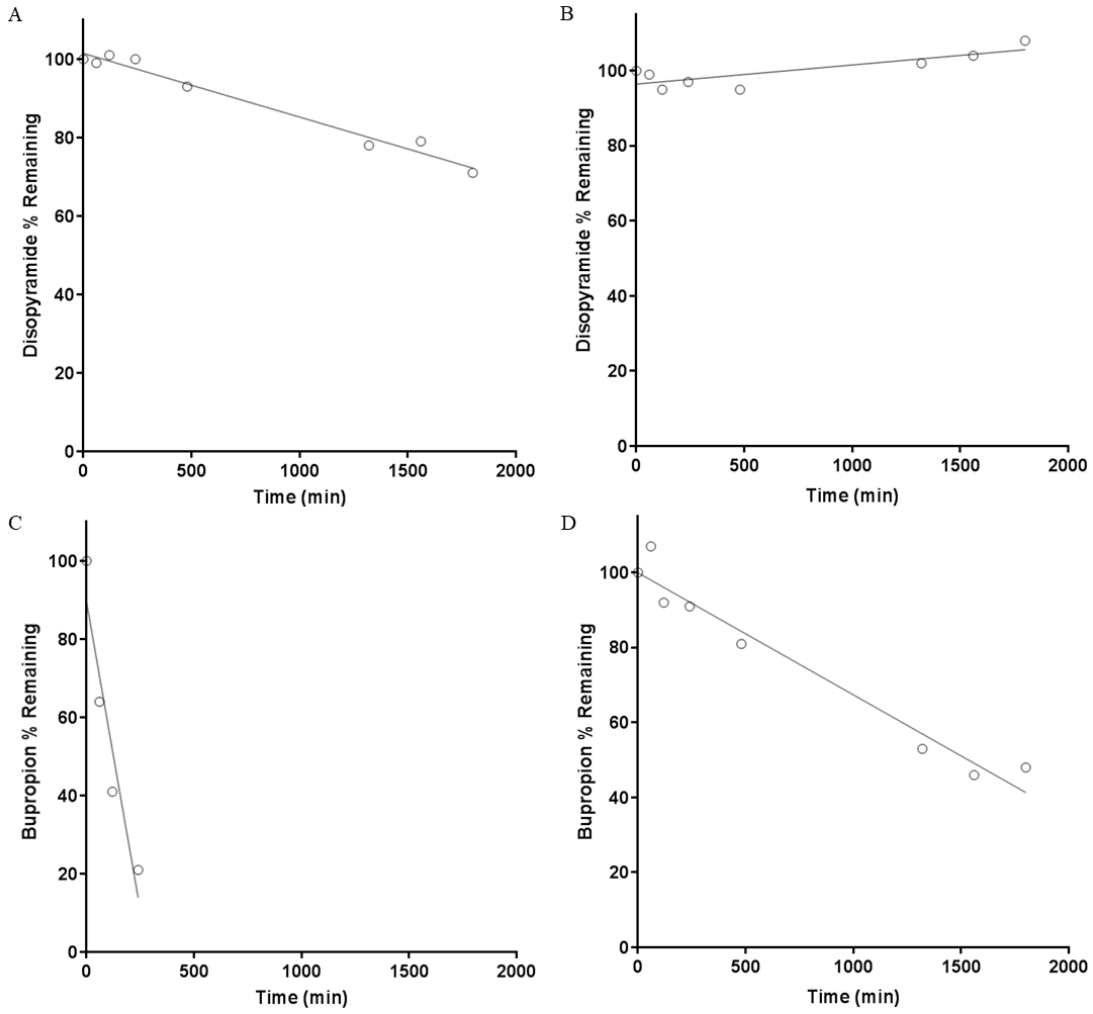

Figure 2

DMD Fast Forward. Published on June 7, 2018 as DOI: 10.1124/dmd.118.081596
This article has not been copyedited and formatted. The final version may differ from this version.

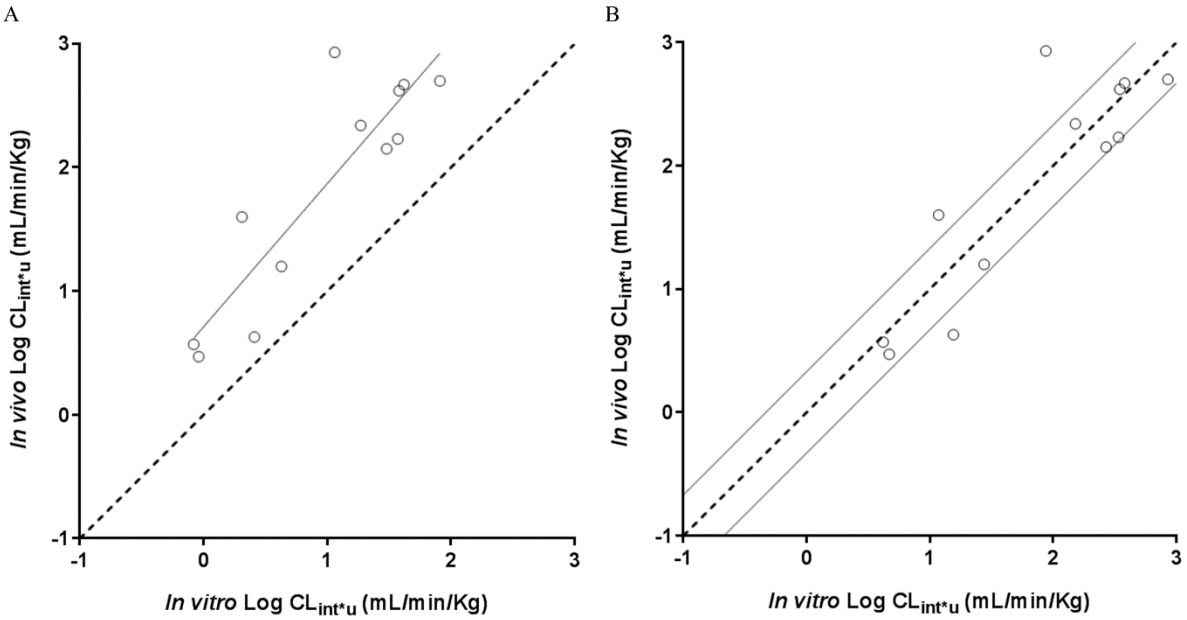

Figure 3

DMD Fast Forward. Published on June 7, 2018 as DOI: 10.1124/dmd.118.081596
This article has not been copyedited and formatted. The final version may differ from this version.

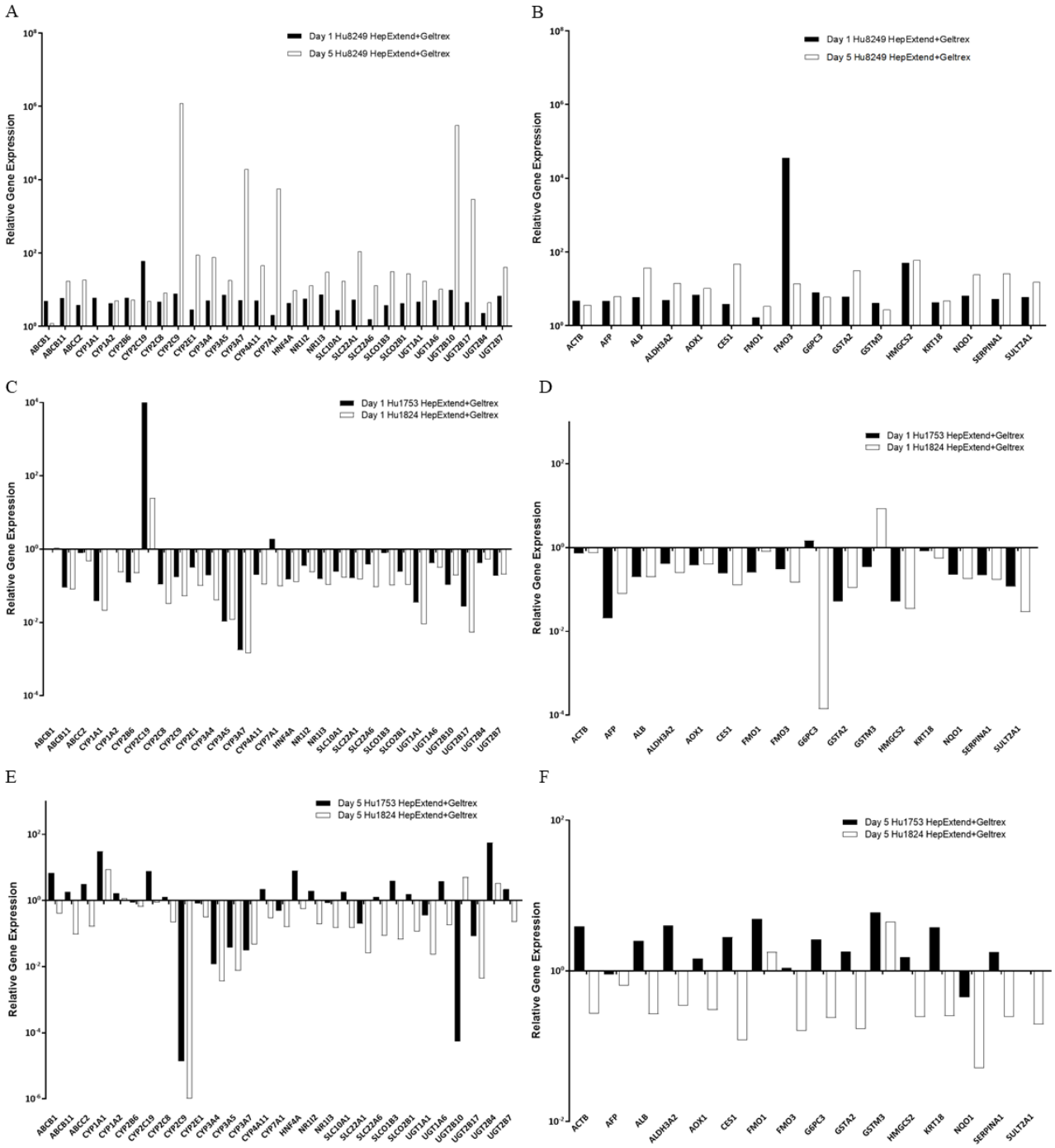

Figure 4

Development and Characterisation of a Human Hepatocyte Low Intrinsic Clearance Assay for Use in Drug Discovery

Paul Lancett, Beth Williamson, Patrick Barton, Robert J Riley

Supplementary Tables

Gene Data

Assay ID	Gene Symbol(s)	Gene Name(s)	Gene Alias(es)	RefSeq(s)	GenBank mRNA(s)	Species
Hs01054797_g1	CYP1A1	cytochrome P450, family 1, subfamily A, polypeptide 1	AHH;AHRR;CP11;CYP1;P1-450;P450-C;P450DX	NM_000499.3	AM233519.1;AK223113.1;M12079.1;AM236046.1;AM233520.1;AM233518.1;BC023019.1;AF040259.1;AY310359.1;AK310810.1;AM233517.1;AK223108.1;K03191.1;AM236047.1;AK313880.1	Human
Hs00167927_m1	CYP1A2	cytochrome P450, family 1, subfamily A, polypeptide 2	CP12;P3-450;P450(PA)	NM_000761.3	BC067428.1;AF182274.1;BC067427.1;M55053.1;BC067424.1;BC067429.1;BC067426.1;Z00036.1;BC067425.1	Human
Hs04183483_g1	CYP2B6	cytochrome P450, family 2, subfamily B, polypeptide 6	CPB6;CYP2B;CYP2B7;CYP2B7P;CYPIIB6;EFVM;IIB1;P450	NM_000767.4	AF182277.1;BC067431.1;X13494.1;BC067430.1;M29874.1;AK301620.1	Human
Hs00258314_m1	CYP2C8	cytochrome P450, family 2, subfamily C, polypeptide 8	CPC8;CYPIIC8;MP-12/MP-20	-	M17398.1	Human
Hs04260376_m1	CYP2C9	cytochrome P450, family 2, subfamily C, polypeptide 9	CPC9;CYP2C;CYP2C10;CYPIIC9;P450IIC9;RP11-208C17.6	NM_000771.3	AK289420.1;M21939.1;M21940.1;M61857.1;D00173.1;AK298458.1;S46963.1;BC125054.1;M15331.1;M61855.1	Human
Hs00426380_m1	CYP2C19	cytochrome P450, family 2, subfamily C, polypeptide 19	CPCJ;CYP2C;P450C2C;P450IIC19;RP11-400G3.4	NM_000769.1	M61854.1	Human
Hs00604506_m1	CYP3A4	cytochrome P450, family 3, subfamily A, polypeptide 4	CP33;CP34;CYP3A;CYP3A3;CYPIIIA3;CYPIIIA4;HLP;NF-25;P450C3;P450PCN1	NM_017460.5;NM_001202855.2	DQ924960.1;DA639071.1;AK298451.1;BC101631.1;X12387.1;AF182273.1;BC069418.1;AJ563375.1;M14096.1;M18907.1;AY606313.2;M13785.1;J04449.1;D00003.1;AK312967.1	Human
Hs04194779_g1	CYP4A11	cytochrome P450, family 4, subfamily A, polypeptide 11	CP4Y;CYP4A2;CYP4AII	NM_000778.3	S67580.1;L04751.1;S67581.1;D26481.1	Human

Hs02576168_g1	CYP2D6	cytochrome P450, family 2, subfamily D, polypeptide 6	CPD6;CYP2D;CYP2D7AP;CYP2D7BP;CYP2D7P2;CYP2D8P2;CYP2DL1;CYPIID6;P450-DB1;P450C2D;P450DB1;RP4-669P10.2	NM_001025161.2;NM_000106.5	BX422592.2;BC075023.2;BC075024.2;AK309600.1;X16865.1;CR456430.1;AY663390.1;BC067432.1;AK308211.1;AB209492.1;X08006.1;M20403.1;X07618.1;BC106757.1;M24499.1;BC066877.1;BC126858.1;BC106758.1	Human
Hs00241417_m1	CYP3A5	cytochrome P450, family 3, subfamily A, polypeptide 5	CP35;CYPIIIA5;P450PCN3;PCN3	NM_000777.3;NR_033809.1;NM_001190484.1	AK299002.1;AK296205.1;J04813.1;BC033862.1;AK313813.1;AK223008.1	Human
Hs99999901_s1	18s rRNA	-	-	-	-	Human
Hs00426361_m1	CYP3A7	cytochrome P450, family 3, subfamily A, polypeptide 7	CP37;CYPIIIA7;P450-HFLA	NM_000765.3	D00408.1;BC067436.1	Human
Hs00559368_m1	CYP2E1	cytochrome P450, family 2, subfamily E, polypeptide 1	CPE1;CYP2E;P450-J;P450C2E	NM_000773.3	AF084225.1;AJ853939.1;AF182276.1;AK290822.1;AJ853940.1;BC067433.1;DQ149222.1;J02625.1;BC067435.1	Human
Hs00167982_m1	CYP7A1	cytochrome P450, family 7, subfamily A, polypeptide 1	CP7A;CYP7;CYPVII	NM_000780.3	BC101777.1;BC112184.1;X56088.1;M93133.1	Human
Hs02511055_s1	UGT1A1	UDP glucuronosyltransferase 1 family, polypeptide A1	BILIQTL1;GNT1;HUG-BR1;UDPGT;UDPGT1-1;UGT1;UGT1A	NM_000463.2	DQ364247.1;JQ699649.1;BC128414.1;AK290834.1;JQ699647.1;JQ699641.1;M57899.1;JQ699643.1;BC128415.1;JQ699642.1;JQ699650.1;JQ699645.1;JQ699638.1;JQ699637.1;AY435136.1;JQ699646.1;JQ686667.1;JQ699640.1;JQ699639.1	Human
Hs01592477_m1	UGT1A6	UDP glucuronosyltransferase 1 family, polypeptide A6	GNT1;HLUGP;HLUGP1;UDPGT;UDPGT1-6;UGT1;UGT1A6S;UGT1F	NM_001072.3	J04093.1;AY435141.1;DQ364250.1;BC019861.1	Human
Hs00426592_m1	UGT2B7	UDP glucuronosyltransferase 2 family, polypeptide B7	UDPGT 2B9;UDPGT2B7;UDPGTH2;UGT2B9	NM_001074.2	AK313190.1;J05428.1;AK223142.1;BC030974.1	Human
Hs00854486_sH	UGT2B17	UDP glucuronosyltransferase 2 family, polypeptide B17	BMND12;UDPGT2B17	NM_001077.3	U59209.1	Human
Hs00161820_m1	SLC10A1	solute carrier family 10 (sodium/bile acid cotransporter), member 1	GIG29;NTCP	NM_003049.3	BC126298.1;AY544127.1;AK314028.1;BC069822.1;BC136355.1;L21893.1;JQ814895.1;BC069799.1;BC074724.2	Human

Hs00427552_m1	SLC22A1	solute carrier family 22 (organic cation transporter), member 1	HOCT1;OCT1;oct1_cds	NM_003057.2;NM_153187.1	AK289887.1;X98332.1;BC126364.1;U77086.1	Human
Hs00251986_m1	SLCO1B3	solute carrier organic anion transporter family, member 1B3	HBLRR;LST-2;LST-3TM13;LST3;OATP-8;OATP1B3;OATP8;SLC21A8	NM_019844.3	AF187815.1;AY342017.1;AJ251506.1;AK055874.1	Human
Hs01030343_m1	SLCO2B1	solute carrier organic anion transporter family, member 2B1	OATP-B;OATP2B1;OATPB;SLC21A9	NM_007256.4;NM_001145211.2	AB026256.1;AF205073.1;BC041095.1;AB020687.1;AL117465.1;AK304783.1;AK302492.1;AK290234.1;AK296079.1;AK294503.1;AK300134.1	Human
Hs01060665_g1	ACTB	actin, beta	BRWS1;PS1TP5BP1	NM_001101.3	AK223055.1;BC013380.2;BC001301.1;AK130062.1;DQ471327.1;AK130157.1;AK223032.1;BC016045.1;BC002409.2;BC004251.1;X63432.1;X00351.1;AK025375.1;AK309997.1;AK222925.1;BC014861.1;BC008633.1;AK304552.1;BC013835.1;BC012854.1;AK225414.1;EF095209.1;AK058019.1	Human
Hs00537914_m1	SLC22A6	solute carrier family 22 (organic anion transporter), member 6	HOAT1;OAT1;PAHT;ROAT1	NM_153278.2;NM_153277.2;NM_153276.2;NM_004790.4	AB009698.1;AJ271205.1;AJ251529.1;AB009697.1;AF104038.1;AF057039.2;AF097490.1;AK055764.1;AK298374.1;BC033682.1;AK091879.1;AF124373.1	Human
Hs00184824_m1	ABCB11	ATP-binding cassette, sub-family B (MDR/TAP), member 11	ABC16;BRIC2;BSEP;PFIC-2;PFIC2;PGY4;SPGP	NM_003742.2	AK302540.1;AF136523.1;AK303050.1;AF091582.1	Human
Hs00184500_m1	ABCB1	ATP-binding cassette, sub-family B (MDR/TAP), member 1	ABC20;CD243;CLCS;GP170;MDR1;P-GP;PGY1	NM_000927.4	AK290159.1;EU852583.1;AB208970.1;M14758.1;AF016535.1;BC130424.1	Human
Hs00166123_m1	ABCC2	ATP-binding cassette, sub-family C (CFTR/MRP), member 2	ABC30;CMOAT;DJS;MRP2;RP11-114F7.2;cMRP	NM_000392.3	X96395.2;U49248.1;U63970.1;BC136419.1	Human
Hs01114267_m1	NR1I2	nuclear receptor subfamily 1, group I, member 2	BXR;ONR1;PAR;PAR1;PAR2;PARq;PRR;PXR;SAR;SXR	NM_003889.3;NM_033013.2;NM_022002.2	AJ009937.1;AJ009936.1;AY091855.1;AF084645.1;HQ709177.1;BC017304.2;AK122990.1;AF084644.1;AF061056.1;HQ692837.1	Human
Hs00901571_m1	NR1I3	nuclear receptor subfamily 1, group I, member 3	CAR;CAR1;MB67	NM_001077474.2;NM_001077476.2;NM_001077471.2;NM_001077472.2;NM_001077470.2;NM_005122.4;NM_001077477.2;NM	AY572818.1;AY572819.1;AY572816.1;AY572817.1;AK303796.1;HQ692841.1;HQ692840.1;HQ692839.1;AY572806.1;HQ692838.1;AY572820.1;BC069626.1;BC121120.1;AY572809.1;AY572826.1;AB307702.1;AY572827.1;AY572810.1;AK310773.1;AY572807.1;AY572815.1;DQ022681.1;AY572808.1;AY572813.1;AK316208.1;HQ709178.1;AK303757.1;AY572814.1;BC121121.1;AY572811.1;AY572812.1	Human

				_001077475.2;NM_001077473.2;NM_001077481.2;NM_001077482.2;NM_001077478.2;NM_001077469.2;NM_001077479.2;NM_001077480.2		
Hs00230853_m1	HNF4A	hepatocyte nuclear factor 4, alpha	HNF4;HNF4a7;HNF4a8;HNF4a9;HNF4alpha;MODY;MODY1;NR2A1;NR2A21;RP5-1013A22.1;TCF;TCF14	NM_001030003.2;NM_001030004.2;NM_001258355.1;NM_000457.4;NM_175914.4;NM_178850.2;NM_178849.2	Z49825.1;X76930.1;HQ692860.1;AY680696.1;X87871.1;BC137539.1;BP274413.1;BC137540.1;X87872.1;AY680698.1;AY680697.1;HQ692869.1;HQ692868.1;X87870.1	Human
Hs00747232_mH	GSTA2	glutathione S-transferase alpha 2	GST2;GSTA2-2;GTA2;GTH2	NM_000846.4	BE795593.1;BE796134.1;AK313601.1;BC002895.2;AK292602.1;M16594.1	Human
Hs00954695_g1	GSTM3	glutathione S-transferase mu 3 (brain)	GST5;GSTB;GSTM3-3;GTM3;RP4-735C1.2	NM_000849.4	EF363096.1;AB209816.1;CR542108.1;J05459.1;BC008790.2;BE392471.1;BC000088.2;AK313444.1;BT019945.1	Human
Hs00234219_m1	SULT2A1	sulfotransferase family, cytosolic, 2A, dehydroepiandrosterone (DHEA)-preferring, member 1	DHEA-ST;DHEAS;HST;ST2;ST2A1;ST2A3;STD;hSTa	NM_003167.3	U08024.1;U08025.1;AK289380.1;L20000.1;BC020755.1;AK313415.1;X84816.1;L02337.1;S43859.1;S43861.1;X70222.1	Human
Hs02512143_s1	NQO1	NAD(P)H dehydrogenase, quinone 1	DHQU;DIA4;DTD;NMOR1;NMORI;QR1	NM_001025434.1;NM_000903.2;NM_001025433.1	BM828301.1;AV729122.1;J03934.1	Human
Hs00166066_m1	ALDH3A2	aldehyde dehydrogenase 3 family, member A2	ALDH10;FALDH;SLS	NM_000382.2;NM_001031806.1	L47162.1;AK025677.1;AK292381.1;BC002430.2;AB208894.1;AK315096.1;CR457422.1;CR749559.1;U46689.1	Human
Hs00266654_m1	FMO1	flavin containing monooxygenase 1	-	NM_002021.1	AK315100.1;AK290113.1;BC047129.1;AK097039.1;AK296198.1;M64082.1	Human
Hs00199368_m1	FMO3	flavin containing monooxygenase 3	FMOII;TMAU;dJ127D3.1	NM_006894.5;NM_001002294.2	AK296105.1;M83772.1;BC032016.1;Z47552.1;AK223166.1;AK298406.1;AK313197.1	Human
Hs00985427_m1	HMGCS2	3-hydroxy-3-methylglutaryl-CoA synthase 2 (mitochondrial)	-	NM_001166107.1;NM_005518.3	AK301594.1;BC044217.1;AK303777.1;X83618.1	Human

Hs00910225_m1	ALB	albumin	GIG20;PRO0883;PRO0903;PRO1341	NM_000477.5	BC036003.1;BC041789.1;V00495.1;AK314794.1;AK308044.1;AY550967.1;AY728024.1;AF542069.1;AK298461.1;CR749331.1;AF190168.1;V00494.1;DQ986150.1;BC034023.1;AY960291.1;HQ537426.1;AY544124.1;AK298437.1;AK292755.1;A06977.1	Human
Hs00275607_m1	CES1	carboxylesterase 1	ACAT;CE-1;CEH;CES2;HMSE;HMSE1;PCE-1;REH;SES1;TGH;hCE-1	NM_001025195.1;NM_001025194.1;NM_001266.4	AK301651.1;AK290623.1;X52973.1;S73751.1;AY268104.1;BC012418.1;BC009706.1;M65261.1;M73499.1;AB025026.1;BC110338.1;M55509.1;AK292209.1;AF177775.1;AB119995.1;AB119996.1;L07764.1;L07765.1	Human
Hs02758991_g1	GAPDH	glyceraldehyde-3-phosphate dehydrogenase	CDABP0047;G3PD;GAPD	NM_002046.4;NM_001256799.1	BU155402.1;BC004109.2;BC013310.2;BC025925.1;BC020308.1;AF261085.1;BC009081.1;DQ403057.1;CR407671.1;M33197.1;EF036498.1;BC029340.1;BC023632.2;X53778.1;AY007133.1;BC001601.1;BC029618.1;BC026907.1;BT006893.1;AB062273.1;AK026525.1;BC083511.1;AK308198.1;X01677.1;M17851.1;AY633612.1	Human
Hs01097800_m1	SERPINA1	serpin peptidase inhibitor, clade A (alpha-1 antiproteinase, antitrypsin), member 1	A1A;A1AT;AAT;PI;PI1;PRO0684;PRO2275;alpha1AT	NM_001127703.1;NM_001127702.1;NM_000295.4;NM_001127701.1;NM_001127700.1;NM_001127707.1;NM_001127706.1;NM_001002235.2;NM_001127705.1;NM_001002236.2;NM_001127704.1	GU727620.1;BX247968.1;DQ682455.1;AK315637.1;BC015642.2;X01683.1;BC070163.1;K01396.1;BX248257.1;M11465.1;AK026174.1;BC011991.1;BX161449.1;X17122.1;X02920.1;BT019455.1	Human
Hs00292720_m1	G6PC3	glucose 6 phosphatase, catalytic, 3	SCN4;UGRP	NM_138387.3	BC021574.1;BC002494.2	Human
Hs00154079_m1	AOX1	aldehyde oxidase 1	AO;AOH1	NM_001159.3	AB046692.1;AK297930.1;BC117181.1;BC117179.1;AK307738.1;L11005.1	Human
Hs00173490_m1	AFP	alpha-fetoprotein	FETA;HPAFP	NM_001134.1	AK297674.1;BC027881.1;V01514.1;AK314817.1;AK297669.1	Human
Hs02827483_g1	KRT18	keratin 18	CYK18;K18;PIG46	NM_199187.1;NM_000224.2	AK308506.1;CD106591.1;BC020982.1;BC000698.2;BC072017.1;AK313988.1;BG753529.1;X12883.1;AK223093.1;BC000180.2;BC004253.1;X12881.1;BC008636.1;BT019412.1;AY762101.1;AK129587.1	Human
Hs02383831_s1	UGT2B4	UDP glucuronosyltransferase 2 family, polypeptide B4	HLUG25;UDPGT2B4;UDPGTH1;UGT2B11	NM_021139.2	AK300084.1;AJ005162.1;BC026264.1;AF064200.1;Y00317.1;AF081793.1	Human

Hs02556282_s1	UGT2B10	UDP glucuronosyltransferase 2 family, polypeptide B10	UDPGT2B10	NM_001144767.1;NM_001075.4	AK222872.1;AK222839.1;AK298432.1;BC113649.1;AK292738.1	Human

Supplementary Table 1. Human genes and identification numbers included in the Taqman gene expression analysis.

Mass Spectrometer Parameters

Compound Name	Monoisotopic Mass	Parent m/z	Daughter m/z	Declustering Potential	Charge	Collision Energy
Bupropion	239.1	240.2	184.1	65	Positive	20
Carvedilol	406.2	407.4	224.2	75	Positive	30
Diazepam	284.1	284.6	193.1	150	Positive	50
Diclofenac	295.0	296.0	214.0	80	Positive	50
Disopyramide	339.2	340.3	239.3	110	Positive	30
Ethinyl Estradiol	296.2	278.8	133.0	50	Positive	20
Imipramine	280.2	281.3	193.2	75	Positive	50
Metoprolol	267.2	268.5	116.2	140	Positive	30
Midazolam	325.1	326.2	291.3	150	Positive	40
Sildenafil	474.2	475.3	283.1	120	Positive	50
Tolbutamide	270.1	271.1	172.2	65	Positive	20
Warfarin	308.1	309.1	163.0	55	Positive	20

Supplementary Table 2. Mass spectrometry methods for all validation compounds.